B. JEŻ [ORCID][1*]

INFLUENCE OF THE COOLING RATE ON THE HETEROGENEITY OF THE STRUCTURE IN THE RAPID QUENCHED FE – BASED ALLOYS WITH THE Si ADDITION

The paper presents the results of research from the analysis of primary magnetization curves for Fe based amorphous alloys. Structural defects in the form of pseudodislocation dipoles occur in amorphous alloys. Using the theory developed by H. Kronmuller called the approach to ferromagnetic saturation, it is possible to indirectly observe internal stresses occurring in the volume of amorphous alloys. The magnetic structure is sensitive to all kinds of inhomogeneities that become visible in the process of high-field magnetization. It has been shown that the cooling rate of the liquid alloy has a great influence on the migration of atoms during the solidification process. Longer time of alloy formation causes more atoms to occupy ordered positions, which results in a change in the distance between the magnetic atoms and a higher degree of structure relaxation. This is indicated by a significant difference in the value of the spin wave stiffness parameter D_{spf}. The structural differences of the alloys were also investigated using a magnetic balance. It has been shown that the cooling rate influences insignificant differences in the course of thermomagnetic curves and the Curie temperature.

Keywords: Amorphous alloys; primary magnetization curve; soft magnetic materials; magnetization in strong magnetic fields

1. Introduction

Technical physics, material engineering or mechanical engineering are looking for new materials that meet the rigorous requirements of industry. Modern alloys based on Zr, Fe, Al or Ti are characterized by excellent mechanical properties [1-3], and in the case of Fe – also magnetic [4,5].

In addition to the chemical composition, the method of manufacturing and further alloy processing plays a key role in creating mechanical and magnetic properties. Amorphous alloys are one of the promising groups of modern functional materials [6-8]. Most production techniques are based on rapid quenched of liquid alloy. This parameter is a key factor when producing amorphous alloys. There are many scientific studies on this topic [9-11]. The vast majority of studies concern the impact of the cooling rate on the glass forming ability and change in the microstructure. This description, however, is extremely difficult due to the microscopic changes in atom positions – SEM and TEM microscopy are often unable to show these changes.

In the case of alloys showing ferromagnetic properties, it is possible to indirectly assess the structure based on the analysis of the magnetic process. The magnetization vector is extremely sensitive to all kinds of obstacles to hinder the magnetization process. According to H. Kronmuller's theory, based on the course of the primary magnetization curve, it is possible to determine the type and amount of defects of the amorphous structure [12-14]. In addition, by analyzing the magnetization course above the approach area to ferromagnetic saturation, it is possible to determine the spin wave stiffness parameter (D_{spf}) [15], which is associated with the matching parameter for magnetization b of the following equation:

$$b = 3.54 g \mu_0 \mu_B \left(\frac{1}{4\pi D_{spf}} \right)^{3/2} kT(g\mu_B)^{1/2} \tag{1}$$

where:

g – gyromagnetic factor,
μ_0 – magnetic permeability of a vacuum,
μ_B – Bohr magneton,
k – Boltzmann's constant,
T – temperature.

Another method enabling the indirect assessment of the amorphous alloys structure is to measure magnetization as a function of temperature in a magnetic field of constant intensity.

[1] CZESTOCHOWA UNIVERSITY OF TECHNOLOGY, FACULTY OF MECHANICAL ENGINEERING AND COMPUTER SCIENCE, DEPARTMENT OF TECHNOLOGY AND AUTOMATION, 19C ARMII KRAJOWEJ STR., 42-200 CZESTOCHOWA, POLAND

* Corresponding author: bartlomiej.jez@pcz.pl

232

In the case of crystalline alloys, the mechanism of transition from ferromagnetic to paramagnetic is well described. As the temperature increases, the crystal lattice is vibrated, which leads to the reconstruction of the magnetic structure – magnetic dipoles cease to set up according to the direction of the applied magnetic field [16]. For crystalline phases, the temperature value at which this phenomenon occurs (Curie temperature, T_C) is a discreet value. In the case of ferromagnetic amorphous alloys, the transition to the paramagnetic state is a more complicated process. It is believed that for amorphous alloys, Curie temperature is not a discreet value but rather a temperature range at which this phenomenon occurs. This is directly related to the chemical and topological ordering of amorphous alloys (or its lack) [17,18]. In microscopic areas of amorphous alloys, the structure may be ordered in a similar way as for the crystalline structure. However, this order is not retained at further distances (the so-called lack of ordering of long-range atoms [18]). The occurrence of such areas is associated with the viscosity of the alloy and the cooling rate. The rapid cooling process hinders the migration of atoms at further distances, which causes fluctuations in the chemical composition in the micro-blade of the amorphous alloy. This means that the transition from Ferro to the paramagnetic is a slightly elongated process and is actually taking place in the micro - areas of alloy. It should be assumed that the fluctuations of the chemical composition and the formation of areas with an atom system similar to the crystalline lattice are associated with the cooling rate (remaining in the amorphous structure). Extremely short allocation time using the Melt – spinning method (cooling rate of 10^5 K/s) hinders the crystallization process to a greater extent than methods using the cooling rate in the range of 10^1-10^3 K/s (for the Injection Casting method [19]). For this reason, it should be assumed, different degrees of relaxation of the structure, which due to the same chemical composition should create the magnetic properties of the alloy.

The purpose of the work is to examine the effect of liquid alloy cooling rate to microscopic changes within the amorphous structure for the selected alloy from the Fe-Co-B group made by various production methods.

2. Experimental

The crystalline alloy $Fe_{65}Co_{9.5}Si_{1.5}Zr_2Hf_2B_{20}$ was created in an arc furnace in an argon atmosphere from ingredients with a purity of 99.99% (for boron 99.9%). Rapid quenched alloy were created using two methods: injection casting and melt – spinning. In two methods, the charge was placed in a quartz melting pot with a hole (diameter of 1 mm). The load was melted using eddy currents. In the Melt Spinning Method, the liquid alloy was injected under the argon pressure on the surface of a copper drum rotating at a speed of 3900 rpm. Bulk alloy samples were created by injecting a liquid alloy into a copper form cooled with water (also under argon pressure). Samples in the form of plates with dimensions of 10 mm × 5 mm × 0.5 mm were obtained. In two cases, identical parameters prevailing in the working chamber

were used: the vacuum level during the pumping of the working chamber, the argon pressure in the working chamber.

The structure of the obtained samples was studied using X-ray diffraction in the range of 30-100° angle 2θ with a 0.02° measuring step and time of 5 seconds exposure. Measurements were carried out for the surface of the ribbon and for the powder obtained in a low-energy crushing process for a bulk alloy. The Bruker Advance 8 diffractometer was used for the tests equipped with a CuKa lamp. The measurement was carried out at room temperature.

Using the lakeshore 7307 vibration magnetometr, the primary magnetization curves and static magnetic hysteresis loops were measured in the external magnetic field up to 2 T. The measurement was carried out at room temperature.

Thermomagnetic curves were measured using the Faraday magnetic balance in the range of room temperature to 850K. The measurement was carried out at a constant intensity of the 0.7 T outer magnetic field. Magnetization curves were registered in the temperature function towards rising temperatures (heating) and in the opposite direction (cooling). The samples were heated at a speed of 10 K/s. Curie temperature for the tested samples was determined on the basis of the equation [20] (2):

$$\mu_0 M_S^{1/\beta} = \left(\mu_0 M_0\right)^{\frac{1}{\beta}}\left(1 - \frac{T}{T_C}\right) \qquad (2)$$

where:

$\mu_0 M_0$ – saturation magnetic polarization for $T = 0K$,

β – critical exponent for a ferromagnetic corresponding to Heisenberg's assumptions and assuming a value $\beta = 0.36$,

T_C – Curie temperature.

3. Results and discussions

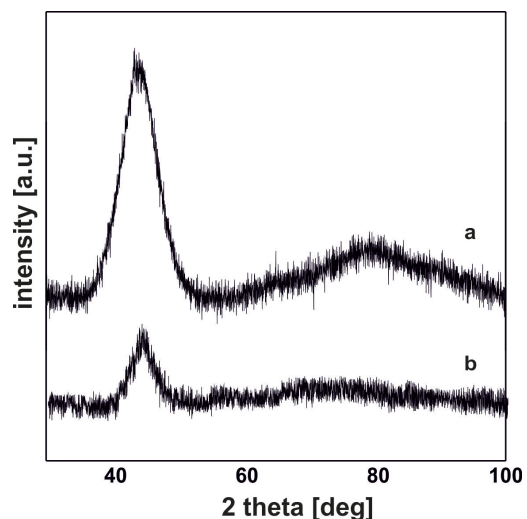The X-ray diffraction patterns measured for the tested samples are shown in Fig. 1.

Fig. 1. X-ray diffraction patterns for the $Fe_{65}Co_{9.5}Si_{1.5}Zr_2Hf_2B_{20}$ alloy: a) ribbon, b) plate

Images of X-ray diffraction are typical as for amorphous materials. Only wide maxima from x-rays reflected from atoms arranged chaotic in alloy volume are visible. For a sample in the form of ribbon, a wide maximum is visible in the range of 35°-55° angle 2θ. For a sample in the form of a plate, this range is 40°-50°. This proves the diverse alloy structure depending on the cooling rate. Fig. 2 includes static magnetic hysteresis loops for tested samples.

The measured loops have different shapes. For ribbon, magnetization reaches the saturation level in a lower value of the external magnetic field compared to the bulk alloy. On the basis of the loop, the value of the coercive field (H_C) was determined and saturation magnetization (M_S), the results were included in TABLE 1.

Primary magnetization was analyzed in accordance with H. Kronmuller's theory. Fig. 3 contains magnetization curves in the area of approach to ferromagnetic saturation.

For a sample in the form of a ribbon, the process of alloy magnetization in the tested area is related to the rotation of the magnetization vector around linear defects with the relationship $D_{dip} < l_H$ (D_{dip} – pseudo-dislocation dipole width) l_H – exchange
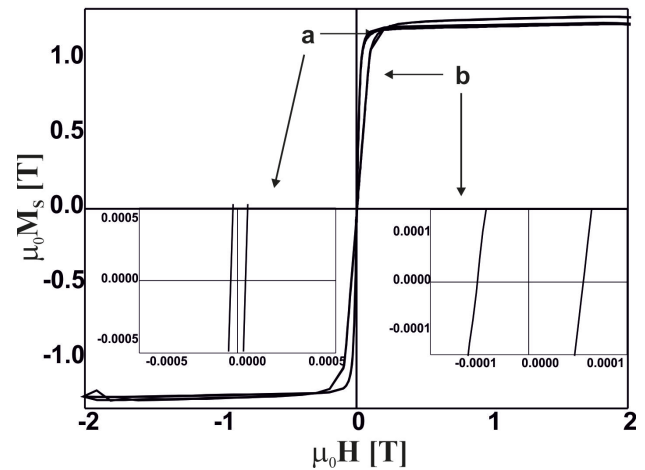

Fig. 2. Static magnetic hysteresis loops for the $Fe_{65}Co_{9.5}Si_{1.5}Zr_2Hf_2B_{20}$ alloy: a) ribbon, b) plate

distances). For a bulk alloy, the magnetization is related to the presence of pseudodislocation dipoles with the relationship $D_{dip} > l_H$. It can therefore be concluded that due to the longer solidification time, the bulk alloy is characterized by a different
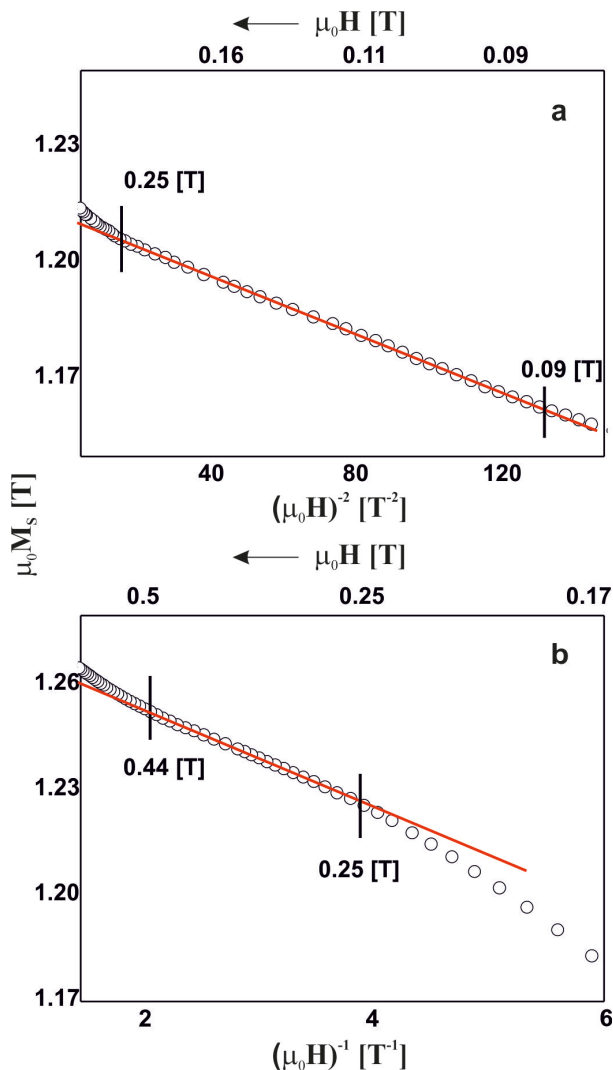

Fig. 3. Magnetisation as a function of $(m_0H)^{-1}$ or $(m_0H)^{-2}$ for the $Fe_{65}Co_{9.5}Si_{1.5}Zr_2Hf_2B_{20}$ alloy. a) ribbon, b) plate
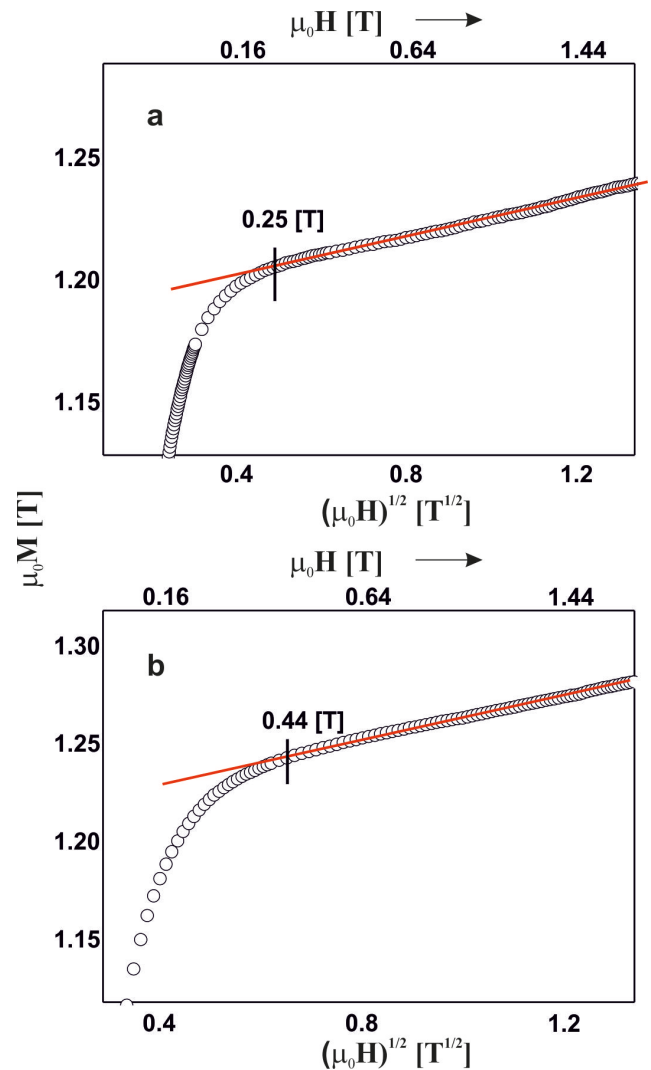
Fig. 4. Magnetisation as a function of $(m_0H)^{1/2}$ for the $Fe_{65}Co_{9.5}Si_{1.5}Zr_2Hf_2B_{20}$ alloy. a) ribbon, b) plate

distribution and size of defects. In this case, longer setting time resulted in a reduction in the size of defects and an increase in the H_C value for the bulk alloy. Fig. 4 shows the magnetization curves above the approach area to ferromagnetic saturation.

The further magnetization of the alloy consists in the damping of thermally excited spin waves. For the sample produced at a higher cooling rate, the Holstein-Primakoff process vapor starts to appear at much lower values of the external magnetic field strength. On the basis of matching to the course of magnetization, parameter b was determined. On its basis, parameter D_{spf} was calculated (TABLE 1).

TABLE 1

Magnetic properties of investigated samples

$Fe_{65}Co_{9.5}Si_{1.5}Zr_2Hf_2B_{20}$	H_C [A/m]	M_S [T]	D_{spf} [meVnm^2]	T_{C1} [K]	T_{C2} [K]
Ribbon	30	1.25	43	647	669
Plate	65	1.28	60	653	670

The ribbon alloy has a H_C value that is twice as low but also a M_S value is lower. First of all, the difference in the value of the D_{spf} parameter is surprising. As is known, this parameter is related to the interactions between magnetic atoms and indirectly describes the distances between the pairs of magnetic atoms Fe-Fe, Co-Co, Fe-Co. A higher value of D_{spf} for a bulk alloy indicates a higher degree of structure relaxation and a reduction in the distance between magnetic atoms. Fig. 5 shows the thermomagnetic curves measured for the tested samples.
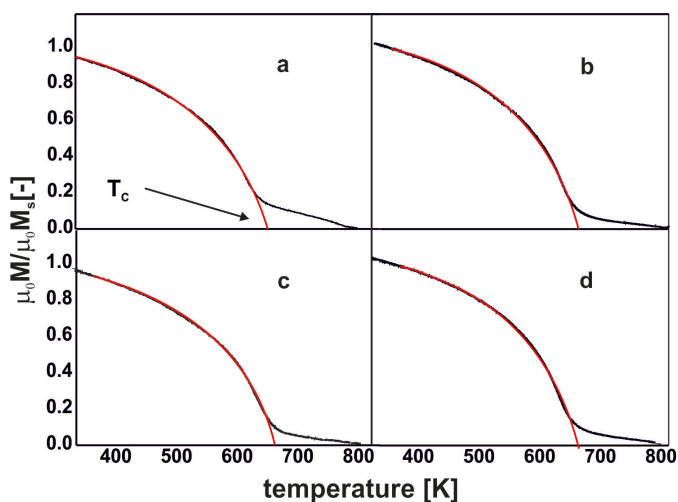

Fig. 5. Thermomagnetic curves for the $Fe_{65}Co_{9.5}Si_{1.5}Zr_2Hf_2B_{20}$ alloy: a) ribbon (heating), b) plate (heating), c) ribbon (cooling), d) plate (cooling)

Also in this case, different courses of the curves are observed depending on the cooling rate. For the alloy produced by melt-spinning, the transition of the sample from ferro to paramagnetic state takes place at a slightly lower temperature. This is due to the shorter solidification time of the alloy and the occurrence of a smaller number of areas with a structure similar to crystalline phases. Interestingly, the return curves (measured in the direction of decreasing temperature values) are almost identical for both tested samples. Relaxation processes occur when measuring at high temperatures (below the crystallization temperature). The configuration of atoms changes, including the distances between magnetic atoms. As a result, it leads to a rearrangement of the magnetic structure, as indicated by a change (increase) in the Curie temperature value (TABLE 1). It should be concluded that the alloy made at the higher cooling rate has a much more disordered structure. When measured at high temperatures, the alloy relaxed to a greater extent than for the sample made at a lower cooling rate.

4. Conclusion

The paper presents the results of research on the effect of cooling rate on the structure and magnetic properties of rapid quenched alloys Fe based alloy. The produced materials are characterized by an amorphous structure, but the different solidification time of the alloy affects the differences in the amorphous phase, which is indicated by changes in the magnetization process in high magnetic fields.

Longer solidification time for bulk samples allows the atoms to occupy ordered positions. Therefore, in bulk amorphous alloys there is an arrangement of short- and medium-range atoms. Further lengthening of the solidification time leads to the ordering of more and more atoms and, as a result, to the long-range ordering of atoms. The presented research results show that by appropriate selection of the cooling rate, it is possible to control the level of structure relaxation and their magnetic properties –without changing the structure to nanocrystalline or crystalline. It should also be stated that the thermal interference, which is the measurement of magnetization as a function of temperature, causes the structure to relax and achieve similar magnetic properties (Curie temperature) despite the presence of different properties in the state after solidification.

REFERENCES

[1] D. Kapinos, M. Szymanek, B. Augustyn, S. Boczkal, W. Szymański, T. Tokarski, J. Lelito, Arch. Metall. Mater. **65** (1), 185-192 (2020).
DOI: https://doi.org/10.24425/amm.2019.131113

[2] A.V. Sandu, M.S. Baltatu, M. Nabialek, A. Savin, P. Vizureanu, Materials **12** (18), 2973 (2019).
DOI: https://doi.org/10.3390/ma12182973

[3] Z. Liu, D. Li, X. Liu, H. Li, X. Huang, Z. Tang, Y. Zou, Arch. Metall. Mater. **65** (2), 677-684 (2020).
DOI: https://doi.org/10.24425/amm.2020.132806

[4] P. Sikora, M. Nabiałek, K. Błoch, J. Gondro, A.V. Sandu, M.M.A.B. Abdullah, A. Kalwik, P. Mousavi, S. Hasani, B. Jez, Acta Physica Polonica A **139** (5), 582-585 (2021).
DOI: https://doi.org/10.12693/APhysPolA.139.582

[5] Y. Han, A. Inoue, F.L. Kong, C.T. Chang, S.L. Shu, E. Shalaan, F. Al-Marzouki, J. Alloy Compd. **657**, 237-245 (2016). DOI: https://doi.org/10.1016/j.jallcom.2015.10.066

[6] F. Hu, C. Yuan, Q. Luo, W. Yang, B. Shen, Journal of Alloys and Compounds **807**, 151675 (2019). DOI: https://doi.org/10.1016/j.jallcom.2019.151675

[7] X. Li, T. Zhang, J. Appl. Phys. **122**, 85103 (2017). DOI: https://doi.org/10.1063/1.4998437

[8] Z. Jaafari, A. Seifoddini, S. Hasani, Metall. Mater. Trans. **50**, 2875-2885 (2019). DOI: https://doi.org/10.1007/s11661-019-05195-z

[9] J. Si, C. Du, T. Wang, Y. Wu, R. Wang, X. Hui, Journal of Alloys and Compounds **741**, 542-548 (2018). DOI: https://doi.org/10.1016/j.jallcom.2018.01.074

[10] P. Rezaei-Shahreza, H. Redaei, P. Moosavi, S. Hasani, A. Seifoddini, B. Jeż, M. Nabiałek, Arch. Metall. Mater. **67** (1), 251-254 (2022). DOI: https://doi.org/10.24425/amm.2022.137498

[11] Y. Geng, Z. Zhang, Z. Wang, Y. Wang, J. Qiang, C. Dong, H. Wang, O. Tegus, Journal of Non-Crystalline Solids **450**, 1-5 (2016). DOI: https://doi.org/10.1016/j.jnoncrysol.2016.07.032

[12] H. Grimm, H. Kronmüller, Physica Status Solidi B **117**, 663-674 (1983). DOI: https://doi.org/10.1002/pssb.2221170228

[13] H. Kronmüller, M. Fähnle, Micromagnetism and the Microstructure of Ferromagnetic Solids, Cambridge University Press, Cambrige, UK 2003.

[14] H. Kronmüller, S. Parkin, Handbook of Magnetism and Advanced Magnetic Materials, Wiley, Hoboken, USA 2007

[15] T. Holstein, H. Primakoff, Phys. Rev. **59** (4), 388-394 (1941). DOI: https://doi.org/10.1103/PhysRev.58.1098

[16] J.M.D. Coey, Magnetism and Magnetic Materials, Cambridge University Press, Cambrige, UK 2009.

[17] K. Błoch, M. Nabiałek, Acta Physica Polonica A **127**, 413-414 (2015). DOI: https://doi.org/10.12693/APhysPolA.127.413

[18] C. Suryanarayana, A Inoue, International Materials Reviews **58** (3), 131-166 (2013). DOI: https://doi.org/10.1179/1743280412Y.0000000007

[19] B. Jeż, Revista de Chimie **68** (8), 1903-1907 (2017). DOI: https://doi.org/0.37358/RC.17.8.5788